SANS study of deformation and relaxation of a comb-like liquid crystal polymer in the nematic phase

A. Brûlet, François Boué, P. Keller, P. Davidson, C. Strazielle, J. Cotton

Classification
Physics Abstracts
61.12E — 61.30 — 61.40

SANS study of deformation and relaxation of a comb-like liquid crystal polymer in the nematic phase

A. Brûlet ([1]), F. Boué ([1]). P. Keller ([1]), P. Davidson ([2]), C. Strazielle ([3]) and J. P. Cotton ([1])

([1]) Laboratoire Léon Brillouin (CEA-CNRS), CE-Saclay, 91191 Gif-sur-Yvette Cedex, France
([2]) Laboratoire de Physique des Solides, Bât. 510, Université Paris XI, 91405 Orsay Cedex, France
([3]) ICS-CRM, 6 rue Boussingault, 67083 Strasbourg, France

Abstract. — A comb-like liquid crystal polymer is stretched and quenched after a certain time in the nematic phase. The conformation of the deformed chain is determined using small angle neutron scattering (SANS) as a function of the temperature of stretching, the stretching ratio and the duration of the relaxation. The scattering data are well fitted to junction affine and phantom network models. Some data are even well fitted by a totally affine model that we call « pseudo affine » because the only parameter, the stretching ratio, is found to be well below the macroscopic stretching ratio. The latter result, never encountered with amorphous polymers, is attributed to the cooperative effects of the nematic phase. We also note that the form factors of the chain in the underformed sample remain similar in the isotropic, nematic and glassy state ; they correspond to a Gaussian chain. The same samples were studied by wide angle X-ray scattering. On one hand, the orientation of the mesogenic groups is found to be parallel or perpendicular to the stretching direction depending on the stretching temperature. This result is discussed as a function of the presence of smectic fluctuations. On the other hand, longer relaxations at constant elongation ratio do not lead to a disorganization of the mesogenic group orientation whereas the polymer chains are partly relaxed.

Introduction.

The aim of this paper is the study of a Comb-Like Liquid Crystalline (CLLC) polymer stretched in the bulk state. Our interest is to compare the deformation of the backbone for a LC polymer in the nematic phase (the conformation of the chain at rest has been already studied [1]) to that of a usual flexible polymer in the amorphous phase [2].

A related problem is the relative orientation of the mesogenic cores with respect to the backbone which is not yet understood in the nematic phase as observed with different methods of orientation and techniques [3-5]. The most common procedure is X-ray diffraction on mechanically oriented samples. A few studies only are made in clearly defined conditions but still [6-10] lead to conflicting results. In addition the backbone can only be assumed to be parallel to the stretching axis.

As regards the backbone, no experiments have been reported yet with stretched CLLC polymers. We were curious to know whether the chain conformation is different from that observed with usual flexible polymers. Concerning the latter the reference model is the affine deformation of the coil with respect to the macroscopic deformation. This behaviour is never observed in the whole range of distance because there is always a loss of affineness [2] related to the relaxation of the material at small distances. This applies for times shorter than the characteristic time of the macroscopic deformation. The relationship between such time τ and distance r is given by the Rouse model [11], $\tau \approx r^4$. In other words there exists a cross-over value, $r^* \approx \tau^{1/4}$, between the deformed behavior at large scale and the isotropic one at small scale. This model is valid for r values smaller than the mean distance between entanglements (the tube diameter D). This description corresponds to the static response of SANS shown in figure 1 where the loss of affineness is clearly seen at a scale where the Rouse regime begins.

For the description of relaxation in amorphous polymers to be complete we recall the behavior at large time. For r greater than D, reptation is assumed in the deformed tube (representing the obstacles due to the other chains) and relaxation occurs mainly from the two end parts of the chain disengaged from the deformed tube extremities. In the reciprocal space, described by the scattering vector q, this corresponds to a scattering function which averages the conformations of parts of chains inside and outside the deformed tube. Thus at each q value corresponds the same distribution of times at variance of the Rouse law $(q \approx \tau^{-1/4})$.

For LC polymers, cooperative phenomena encountered in the nematic phase should involve the polymer at all scales (the mesogenic groups align the backbone which in turn align the mesogenic groups, and so on). A smaller scale of correlation times is expected in this global process. We think that this mechanism would not allow the existence of the Rouse regime where chains relax individually. Thus the scattering curves could display an affine deformation.

Small Angle Neutron Scattering (SANS) is the main tool for the determination [12] of the backbone conformation from a mixture of fifty percent of deuterated and protonated polymers. We will use it here in order to determine the backbone response of an *uncrosslinked* LC polymethacrylate stretched in its nematic state. The corresponding mesogen orientation will be evaluated from X-ray experiments with *the same sample*.

The paper is organized as follows : in section 1 the preparation of the sample and neutron and X-ray set ups are described. Then in section 2 we recall the phantom network model which allows us to calculate the scattering function of a mixture of polydisperse polymers in the stretched state. In section 3 we describe the results obtained with an undeformed sample whereas in section 4 the results of preliminary experiments obtained with three temperatures of deformation are given. Then the variation with the deformation ratio and the variation of the relaxation durations are shown in section 5. Section 6 is devoted to a general discussion of the results.

1. Experimental.

1.1 SYNTHESIS OF POLYMERS. — The side chain liquid crystal polymethacrylates (PMA_H-CH_3 and PMA_D-CH_3),

$$-(CR_2{-}\underset{\underset{CO_2{-}(CH_2)_6{-}O{-}\phi{-}CO_2{-}\phi{-}CH_3}{|}}{\overset{\overset{CR_3}{|}}{C}}){-}$$
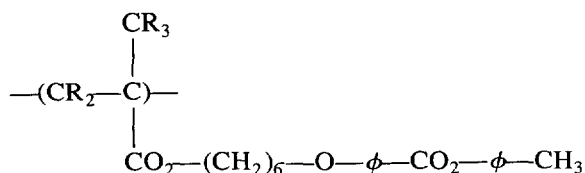
where R is either H or D, were obtained by free radical polymerization of corresponding methacrylate monomers in solution [13]. The molecular weight distributions were determined by size exclusion chromatography with light scattering on line (SEC-LS) at Institut Charles Sadron, Strasbourg. The average molecular weight M_w of the polymer PMA_HCH_3 is 217 000 with a polydispersity M_w/M_n of 2.7. For PMA_DCH_3, M_w is 336 000 and M_w/M_n = 3.7.

These polymers present a nematic phase lying in between the nematic isotropic transition temperature T_{IN} = 82 °C and the glass transition : T_g = 45 °C [14].

This rather large nematic range allows deformations in a wide range of temperatures and quenching in the glassy nematic state.

1.2 SAMPLE PREPARATION. — A mixture of hydrogenated and deuterated PMA_-CH_3 was prepared by dissolving the two polymers at 50 : 50 weight ratio in chloroform. After drying under vacuum at room temperature, the powder was then moulded at 130 °C into strips of initially $18 \times 9 \times 1$ mm³. The samples have been stretched rapidly (elongation time t_S between 1 and 80 s) by an elongation ratio λ (from 1.3 to 3) at a temperature $T_{NI} > T_D > T_g$ in a silicon oil bath, then maintained at constant length and constant temperature for a certain relaxation time t_R before being quenched in the glassy state at room temperature [15]. Elongation ratios were determined by measuring the distances between reference marks drawn on the sample before and after deformation in the three principal directions. We have checked that the macroscopic deformation was

$$\mathbf{r} \to E \cdot \mathbf{r} \qquad E = \begin{pmatrix} \lambda^{-1/2} & 0 & 0 \\ 0 & \lambda^{-1/2} & 0 \\ 0 & 0 & \lambda \end{pmatrix}$$

giving consistent λ values within $\Delta\lambda/\lambda$ = 0.1.

A sample is characterized by t_S the duration of stretching, λ, t_R and T_D. We consider this deformation as an instantaneous one followed by a relaxation of duration $t_S + t_R$ ($t_S \ll t_{ter}$ where t_{ter} is the largest relaxation time). Since the characteristic relaxation times of the polymer decrease with increasing temperature, t_S and t_R have been chosen conveniently shorter at higher T_D. These experimental parameters for each sample are given together with our results in section 4 and 5. Section 5 also involves samples which have been relaxed, then measured and relaxed again (by dipping them again in the bath), measured again, and so on.

The stretching temperatures are 55, 67, and 77 °C. For amorphous polymers it is usual to observe that the sample is able to recover its initial length for $t \ll t_{ter}$; as is well known, this occurs because entanglements then play the same role as crosslinks in a rubber. Here the reversibility of the deformation is a function of temperature : at 55 and 67 °C, the sample is able to recover its initial length within a few percent whereas, at 77 °C, the recovery is far from complete (the deformation better ressembles a flow). In these polymers, the origin of « entanglements » is not yet understood.

1.3 NEUTRON EXPERIMENTS. — The measurements were performed on the PAXY spectrometer at LLB (Orphée reactor, CE-Saclay). The distance between the sample and the multidetector (128 × 128 cells of 5 × 5 mm²) was 3.2 m and the neutron wavelength was 10 Å. The scattering vector range was $7 \times 10^{-3} < q < 6.4 \times 10^{-2}$ Å^{-1}

For the undeformed sample, the regrouping of the isotropic scattering was annular. For anisotropic samples, the regrouped cells were selected among rectangles of 11 cells of width aligned along the stretching direction and 7 cells in the perpendicular direction. Each scattering was corrected from transmission, sample thickness and detector efficiency (using 1 mm water cell). The incoherent background due to the H nuclei in the labelled sample calculated from the

signal of the undeformed PMA_HCH_3 sample was then subtracted. Absolute calibration of SANS data was obtained by direct measurement of the incident beam flux [16]. The differential scattering cross sections, $I_{\parallel}(q)$ and $I_{\perp}(q)$ are expressed in cm^{-1}

1.4 X-RAY EXPERIMENTS. — The X-ray diffraction experiments were carried out with an already described apparatus [17]. The X-ray beam is produced by a rotating copper anode generator equipped with a microfocus. A nearly parallel monochromatic ($\lambda_{CuK_\alpha} = 1.541$ Å) beam is obtained by reflection from a bent graphite slab. The beam size is about 1 mm^2 at the sample level. The scattered X-rays were collected either with a two-dimensional proportional counter [18], for test purposes, or with photographic plates. The scattering vector range was $10^{-1} < q < 3$ Å^{-1}

It is worth noting that samples contained in capillary tubes of 1.5 mm diameter could not be aligned (as checked by X-ray diffraction) in a magnetic field of 1.7 T by the usual procedures. Moreover, fibers were drawn with a pair of tweezers from the isotropic melt. These fibers observed in the polarizing microscope were quite birefringent, but their X-ray diffraction patterns were isotropic.

2. Models for scattering functions.

2.1 MIXTURES OF H AND D CHAINS. — According to the random-phase approximation (RPA), the coherent neutron scattering $S_T(q)$ from a mixture of ϕ_D labelled polymer chains and $(1 - \phi_D)$ matrix hydrogenated chains is given by [19] :

$$\frac{1}{S_T(q)} = \frac{1}{\phi_D S_D(q)} + \frac{1}{(1 - \phi_D) S_H(q)} - 2\chi$$

where χ is the interaction parameter between D and H monomer units, $S_D(q)$ and $S_H(q)$ are the form factors of the two types of chains.

Since the molecular weight distribution $f(N)$ of polymers is relatively large, generalization of this equation is used following the RPA [19] :

$$\frac{1}{S_T(q)} = \frac{1}{\phi_D \langle S_D(q) \rangle} + \frac{1}{(1 - \phi_D) \langle S_H(q) \rangle} - 2\chi \qquad (1)$$

defining

$$\langle S_i(q) \rangle = \frac{1}{\int f_i(N) \, dN} \int f_i(N) S(q) \, dN \; ; \quad i = H \text{ or } D \,. \qquad (2)$$

In our calculation $f_i(N)$ is deduced from SEC-LS measurements. Previous SANS experiments on that kind of polymers do not report any noticeable effect of χ [1c 23]. For our mixture of homopolymers of comparable and not very high molecular weights, the influence of χ can be negligible.

At rest, if the chain configurations are ideal, $S_D(q)$ and $S_H(q)$ can be expressed in terms of the Debye function $D(q)$:

$$S(q) = ND(Nq^2 a^2/6)$$

$$D(x) = (2/x^2)\{\exp(-x) + x - 1\} \; ; \quad x = q^2 R_g^2; \quad R_g^2 = \frac{Na^2}{6} \qquad (3)$$

where R_g is the radius of gyration.

2.2 DEFORMED CHAINS. — The affine deformation discussed in the introduction corresponds to the following form factors :

$$S_\parallel (q) = ND(\lambda^2 x) ; \qquad S_\perp (q) = ND(x/\lambda) . \tag{4a}$$

At large q, $q^2 S(q)$ for both directions reach a plateau of levels :

$$q^2 S_\parallel (q) = \frac{12}{a^2 \lambda^2}, \quad q^2 S_\perp (q) = \frac{12 \lambda}{a^2} \tag{4b}$$

A more realistic model takes into account the loss of affineness to the macroscopic deformation when the scale decreases from the macroscopic dimension of the sample to the undeformed scale of the monomer. This behaviour, as discussed in the introduction, is predicted by the Rouse model. it is also a general feature of rubber elasticity. Both can be described schematically by considering chains linked to fixed points but free to rearrange between them. In a first model cross links can be displaced affinely under deformation. This junction affine model [20] has been slightly modified in a phantom network model [21] where the junctions (crosslinks) are assumed to fluctuate around their affinely deformed mean positions. An important idea of the latter model is that the fluctuations of the junctions are independent of the strain. These models developed for networks have also been used for melts in modern theories where entanglement points replaced cross links. They can thus be described by a chain inside a deformed tube for which $S(q)$ has been given by Warner and Edwards [22] which corresponds to an affine deformed chain of Gaussian blobs of p monomers. The scattering can be expressed as a single sum :

$$S_\varphi (q) = \frac{S_\varphi (0)}{N^2} \times$$

$$\times \left\{ N + 2 \sum_{k=1}^{k=N-1} (N-k) \exp \left[- \left(\frac{q^2 a^2}{6} \right) \left(\alpha^2 k + p(1 - \alpha^2) \left(1 - \exp \left(-\frac{k}{p} \right) \right) \right) \right] \right\} \tag{5}$$

α is the deformation along the vector **q** i.e.

$$\alpha^2 = \lambda^2 \cos^2 \varphi + \frac{1}{\lambda} \sin^2 \varphi$$

where φ is the angle between **q** and the stretching axis. In the following we define $S_\parallel (q) = S_0(q)$ and $S_\perp (q) = S_{90}(q)$.

We have performed numerical evaluations of the intensity scattered by a mixture of deuterated and hydrogenated polydisperse chains following equations (5) and (1). $S_T(q)$ can be calculated for different values of the deformation ratio and molecular weights of elementary sequences between entanglements (corresponding to different numbers of monomer units per mesh).

2.3 REPRESENTATION OF $S_T(q)$. — For large q values ($qR_{gapp} \gg 1$) the variation of $S_T(q)$ is independent of the polydispersity, as can be clearly seen using the Kratky representation, $q^2 S_T(q)$ versus q, which gives a plateau in this intermediate q range (see Fig. 1). This representation allows us to focus on the loss of affineness visible at large q. Thus the Kratky representation will be used in the following.
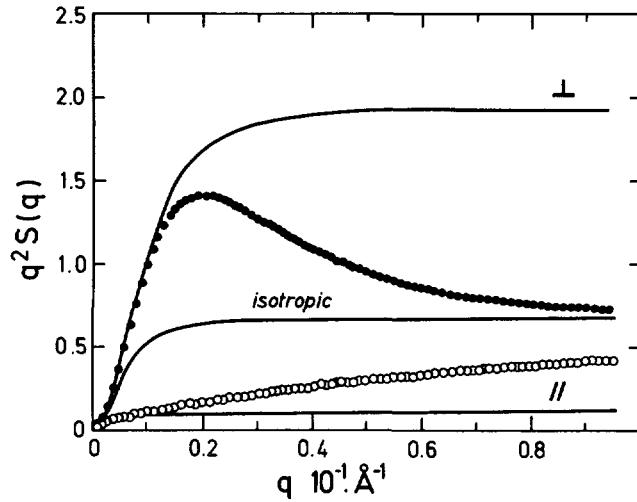
Fig. 1. — Representation of $q^2 S(q)$ versus the scattering vector q for the calculated form factors $S(q)$ for a totally affine model $\lambda = 3$ (full lines upper ($\perp$) and lower curves $\parallel$) and for a phantom network model $\lambda = 3$, $p = 100$ (see Eq. (5)); ($\bigcirc$) $\parallel$ curve; ($\bullet$) $\perp$ curve). The polymer is a polystyrene chain of 7 000 units. The isotropic scattering is shown on the medium full line.

3. Results for the undeformed sample.

Undeformed samples were studied in two ways :

(i) in a quartz cell at three temperatures 100 °C, 67 °C and 42 °C ;
(ii) annealed at about 85 °C for 10 mn and then quenched to room temperature.

The corresponding scattering curves are very similar and give the same value for the apparent radius of gyration $R_{gapp} = 101 \pm 4$ Å obtained from the Zimm representation :

$$S_T^{-1}(q) = S_T^{-1}(0)(1 + q^2 R_{gapp}^2/3) ; \quad qR_{gapp} \leq 1 . \tag{6}$$

At large q, the curves approach the plateau (see Fig. 2) characteristic of a Gaussian conformation in the Kratky representation. This representation is very sensitive to the background subtraction and to the difference of densities of the phases. This probably explains the small differences ($\pm 5 \%$) observed between the scattering (i) and (ii) (curves not shown here).

The scattered intensity for sample (ii) has been fitted to a form factor of a mixture of polydisperse Gaussian chains according to equations (3) and (1). In our calculations we have used the normalized weight distribution functions of the polymers measured by SEC-LS. By fitting experimental data to equation (1) we determine the following relation between R_g and the molecular weight M

$$R_g = (0.17 \pm 0.01) M^{1/2}$$

This value of 0.17 is to be compared to that of 0.24 found with another polymethacrylate [1c, 23].

In figure 2, we can observe, at the intermediate q values, a little discrepancy between the data and the calculated points. This could be attributed to a non-zero (but small) value of the Flory-Huggins interaction parameter between H and D species the influence of which increases
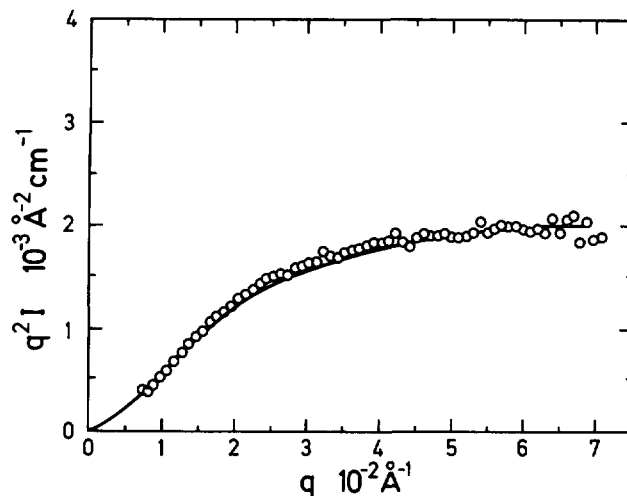
Fig. 2. — Representation of $q^2 I(q)$ *versus* the scattering vector q for the scattering intensity $I(q)$ by the quenched liquid crystal polymer at rest. The full line is a best fit to Gaussian chains (Eqs. (1) and (3)).

with the molecular weight of the polymers. However, this effect is not very significant and does not change the main conclusions of this study.

In summary a Gaussian conformation is adopted by the LC chains in the isotropic phase and is kept after quenching to room temperature. It is a remarkable result in particular in the nematic phase.

4. Exploration experiments at different temperatures.

In this section, we present neutron and X-ray scattering data for samples deformed ($\lambda = 3$) inside the nematic phase at three temperatures : 55 °C (close to the glass transition $T_g = 45$ °C), 67 °C and 77 °C (close to the nematic-isotropic phase transition).

We first discuss the SANS data shown in figure 3. The most striking result for $T_D = 55$ °C (Fig. 3a) and 67 °C (Fig. 3b) is that no loss of affinity appears for large q values. i.e. the curves in parallel and perpendicular directions do not tend to join the isotropic curve, as is usually observed for amorphous polymers (see Fig. 1) for similar of values q and $t_R + t_S$. In particular $q^2 I_\perp (q)$ does not show any maximum but seems to reach a plateau. This can be made quantitative by fitting simultaneously both scattering curves $I_\parallel (q)$ and $I_\perp (q)$ by equations (1) and (5). The following procedure is used : the value of $S(0)$ is obtained from the extrapolation to $q = 0$ of $I_\perp^{-1}(q)$ *versus* q^2 in the Guinier range which is very accessible in the perpendicular direction. Then this value is introduced into the calculation of $I_\perp (q)$ and $I_\parallel(q)$. The fit consists in the determination of λ and p using the relation $R_g = 0.17 \sqrt{M}$ for the radii of gyration.

The best values of λ and p are obtained by visual comparison of the calculated curves with the experimental ones in both directions simultaneously.

From another point of view the values of $S(0)$ obtained for each sample display differences (below 20 % relatively to the value of the isotropic sample) which we attribute to errors in the determination of the thickness of the stretched samples.

The results for values of λ and p are summarized in table I where the values of R_{gapp} are also given (see Eq. (6)) for both directions. Figure 3 shows the corresponding fit for
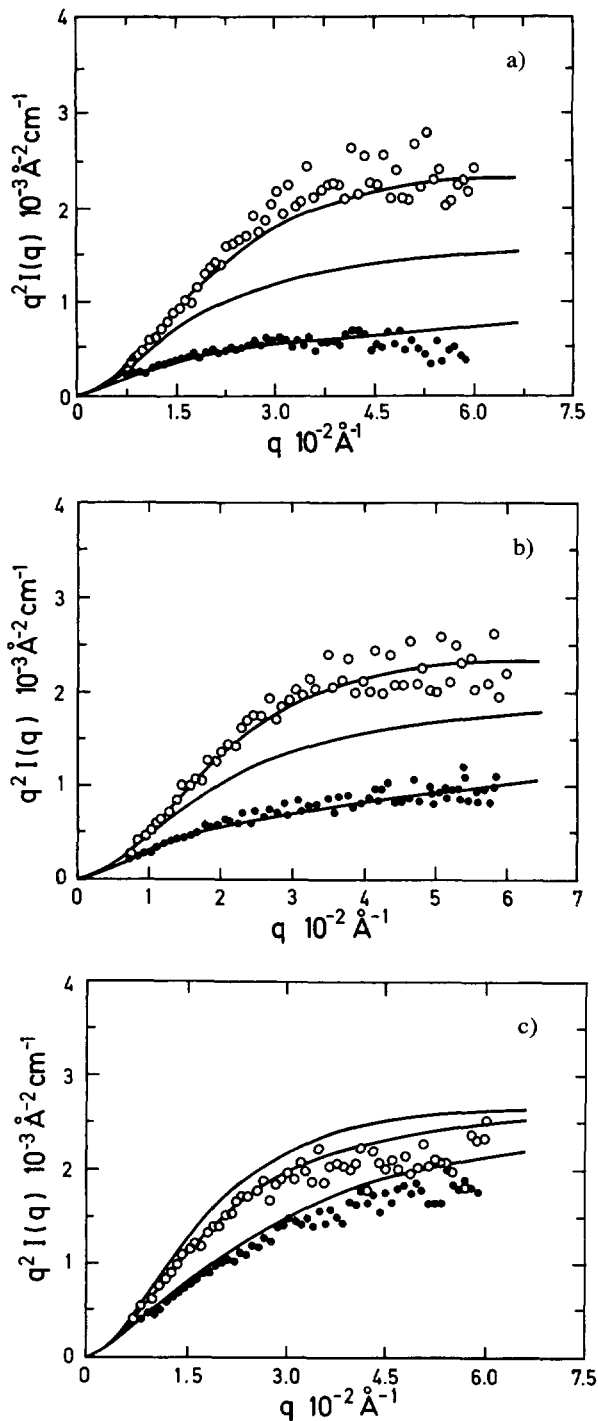
Fig. 3. — Representation of figure 2 for stretched liquid crystal polymers (●) corresponds to the parallel direction (O) to the perpendicular one. Upper and lower full lines are the best fit (see Eqs. (1) and (5)). The intermediate full line corresponds to the isotropic case. The values of the parameters are : a) $\lambda = 3$, $T = 55$ °C, $\lambda_p = 1.9$ $p = 10$. b) $\lambda = 3$, $T = 67$ °C, $\lambda_p = 1.7$ $p = 15$. c) $\lambda = 3$, $T = 77$ °C, $\lambda_p = 1.8$ $p = 200$.

Table I. — *Characteristics of samples and neutron results.* λ *is the elongation ratio,* T_D *the temperature of deformation,* t_S *and* t_R *the durations of the stretching and of the relaxation,* R_{gapp} *is the radius of gyration obtained from a Zimm plot.* λ_p *and* p *are parameters of fits to equation* (5).

λ	T_D (°C)	t_S (s)	t_R (s)	$R_{gapp\parallel}$ (Å)	$R_{gapp\perp}$ (Å)	λ_p	p
3	55	230	0	170 ± 10	72 ± 5	1.9 ± 0.5	10 ± 5
3	67	76	0	155 ± 10	81 ± 5	1.7	15
3	77	5	0	105 ± 5	100 ± 5	1.8	200
1.3	55	22	0	125 ± 5	90 ± 3	1.2 ± 0.05	5 ± 2
1.6	55	80	0	146 ± 5	83 ± 3	1.5	10
2	55	86	0	152 ± 7	78 ± 3	1.6	20
3	55	76	0	170 ± 10	70 ± 3	2.05	10
3	55	76	400	—	—	1.55	35
3	55	76	1 300	110 ± 10	84 ± 5	1.35	55

the three temperatures. Figure 3a corresponds to $T_D = 55$ °C : a rather good fit is obtained with an effective value of λ : $\lambda_p = 1.9$ and $p = 10$. In practice it is very close to a totally affine deformation ($p = 1$ or Eq. (4a)) with a λ_p value slightly lower $\lambda_p = 1.7$. Let us notice that these effective values are *very much lower than the applied deformation of 3*.

Figure 3b is quite similar to figure 3a ; the phantom model gives $\lambda = 1.7$ with $p = 15$ whereas the totally affine models gives $\lambda_p = 1.55$ ($p = 1$). For both samples the relevant parameter is λ_p and not p. Figure 3c corresponds to a different behaviour since a large value of p is found $p = 200$ for $\lambda_p = 1.8$. This forbids any fit to an affine model. The latter result is obtained at a temperature of 77 °C which is relatively close to the nematic-isotropic transition. In figure 3c we note that the simultaneous fit of $q^2 I_\parallel$ and $q^2 I_\perp$ is not possible. The calculated curve for sample at rest fits better the data in the perpendicular direction. It may be because the deformation is now (77 °C) closer to a viscoelastic flow.

In summary, when the temperature is increased from the glass transition to the nematic-isotropic transition, an increase of the loss of anisotropy of the chain is observed, *mainly in a decrease of* λ_p. A significant value of p is observed only at the highest temperature.

The X-ray diffraction patterns of the same samples are shown in figure 4. All these patterns show the usual wide angle diffuse ring [17] (A) which hints at the fluid nature of the mesophase. This diffuse ring is due to the lateral interferences among mesogenic cores and, when it is anisotropic, the direction of its maximal intensity is perpendicular to the preferred orientation of the mesogenic cores. Therefore, figure 4a shows that they are oriented perpendicular to the stretching direction at 55 °C, figure 4c shows that the side chains are oriented parallel to the stretching direction at 77 °C and figure 4b shows that they are completely unoriented at 67 °C (even at high stretch $\lambda \approx 3$). Furthermore, the width $\Delta\theta^{1/2}$ (FWHM) of the diffuse ring is a useful parameter (see the discussion in Ref. [17]) to

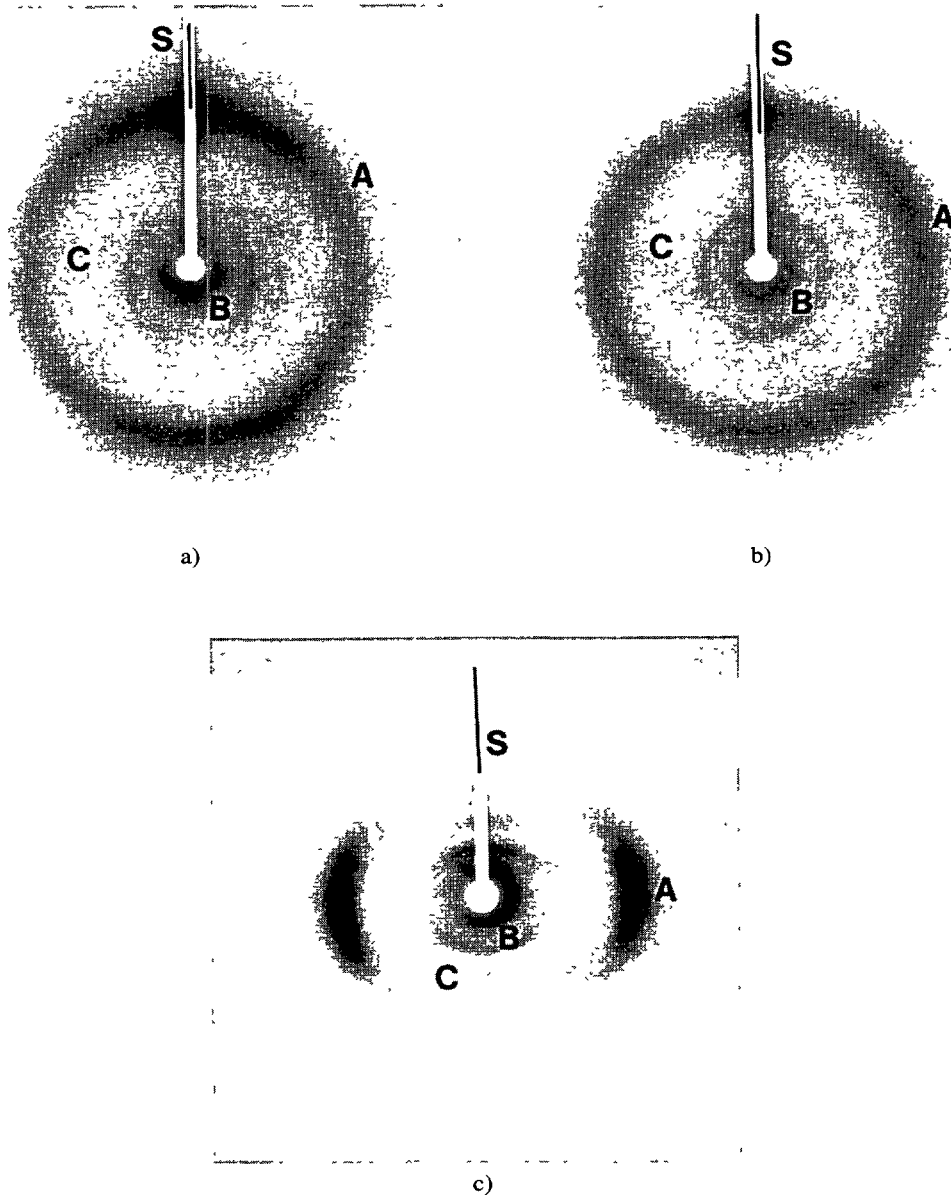a)   b)

c)

Fig. 4. — X-ray diffraction pattern of samples stretched at a) $T_D = 55$ °C, side chains are perpendicular to the stretch. b) $T_D = 67$ °C, side chains are unoriented, c) $T_D = 77$ °C, side chains are parallel to the stretch. (A) Wide angle diffuse ring, (B) sharp reflection, (C) in addition, a set of diffuse lines is classically due to short range one-dimensional correlations [28]. This confirms in each case the orientation of the side chains. ($\lambda_{CuK_\alpha} = 1.541$ Å, sample-film distance 80 mm) S is the stretching direction.

characterize the orientation degree of the side chains. The smaller this width, the better oriented is the side chains. One cannot use here the usual treatment [24, 25] of the wide angle diffuse ring to derive the nematic order parameter because the samples are not monodomains. Figure 4a leads to the value of $\Delta\theta^{1/2} \approx 70°$ which represents a fair alignment of the side chains

in the plane perpendicular to the stretch. The rather low value $\Delta\theta^{1/2} \approx 50°$ obtained from figure 4c shows that the side chains are well-oriented along the stretching direction.

Let us notice that the complementary techniques, small angle scattering (SANS) and wide angle X-ray scattering (WAXS), give totally different results : SANS shows that the chain backbone is elongated along the stretching axis while WAXS shows that the orientation of the mesogenic cores is parallel to the stretching axis only at high temperatures (see the discussion of Sect. 6).

Let us now turn to the central part of the X-ray diffraction patterns. Figures 4a-c actually show the diffraction patterns of aged samples, stored at room temperature for typically a few months. These patterns show in their central part a sharp reflection (B) at $q = \dfrac{2\,\pi}{24.7}\,\text{Å}^{-1}$ located on the meridian of the oriented patterns. This sharp reflection proves that the aged samples (whatever their orientation state) are no longer in a nematic state but, at least in part, in a smectic state instead. The geometry of reciprocal space and also the comparison with the length $\ell \approx 23.1$ Å of a side chain in its most extended conformation imply that the smectic phase is of the A type. The X-ray patterns not presented here of freshly samples do not show these sharp reflections but they display diffuse spots instead. This means that the fresh samples are still in a nematic state subject to SmA fluctuations, but they slowly evolve with time and turn to a SmA state within a few months. This situation is not uncommon in the field of mesomorphic side chain polymers.

5. Deformation and relaxation at low temperature.

The deformations of samples discussed now were done at 55 °C following two procedures. The first one consists in stretching each sample at different elongation ratios and letting all samples relax during the same time. The second one consists in stretching the sample at $\lambda = 3$ and performing successive measurements of the scattering for different increasing t_R values. $T_D = 55$ °C was chosen in order to be in the vicinity of T_g and because it allows an easy deformation in the time range of the stretching machine. Moreover the range of t_R is well suited to the characteristic relaxation times of the chain in the sample.

The time temperature superposition principle [26] generally accepted for amorphous polymers in the vicinity of T_g will not be used here since different temperatures may correspond to different mesophases.

5.1 VARIATION WITH THE ELONGATION RATIO. — The elongation ratios are $\lambda = 1.3$, 1.6, 2.0, and 3.0. The values of $R_{\parallel \text{app}}$ and $R_{\perp \text{app}}$ obtained using equation (6) and the Zimm representation are given in table I. The data $q^2 I(q)$ are shown in figure 5a ($\lambda = 1.3$), 5b ($\lambda = 1.6$) and 5c ($\lambda = 2$) together with the best fits to the phantom model (Eq. (5)) following the procedure described above. The corresponding values of λ_p and p are given in table I. Here also the curves are well fitted with small values of p and λ_p, values which are below the applied elongation ratio λ. λ_p is an increasing function of λ but the ratio λ_p/λ decreases with λ. The values of λ_p are also consistent with those deduced from the ratios $R_{g\text{app}}/R_{g\text{iso}}$.

X-ray measurements have been performed on these samples. They display the same orientation as that of the sample stretched at 55 °C, discussed in the former section, i.e. the mesogenic cores are perpendicular to the stretching axis. More precisely, at a given temperature (55 °C), the orientation improves with the strain : there is no measurable orientation for $\lambda = 1.3$ whereas $\Delta\theta^{1/2} = 90°$ for $\lambda = 2$ and $\Delta\theta^{1/2} = 70°$ for $\lambda = 3$.

5.2 INFLUENCE OF THE RELAXATION. — The same sample ($\lambda = 3$) has been observed after each of three successive relaxations of duration $(t_S + t_R) = 76$ s, 476 s and 1 376 s. The data for $t_R = 76$ s are very close to that of figure 3a obtained under very similar conditions. The data
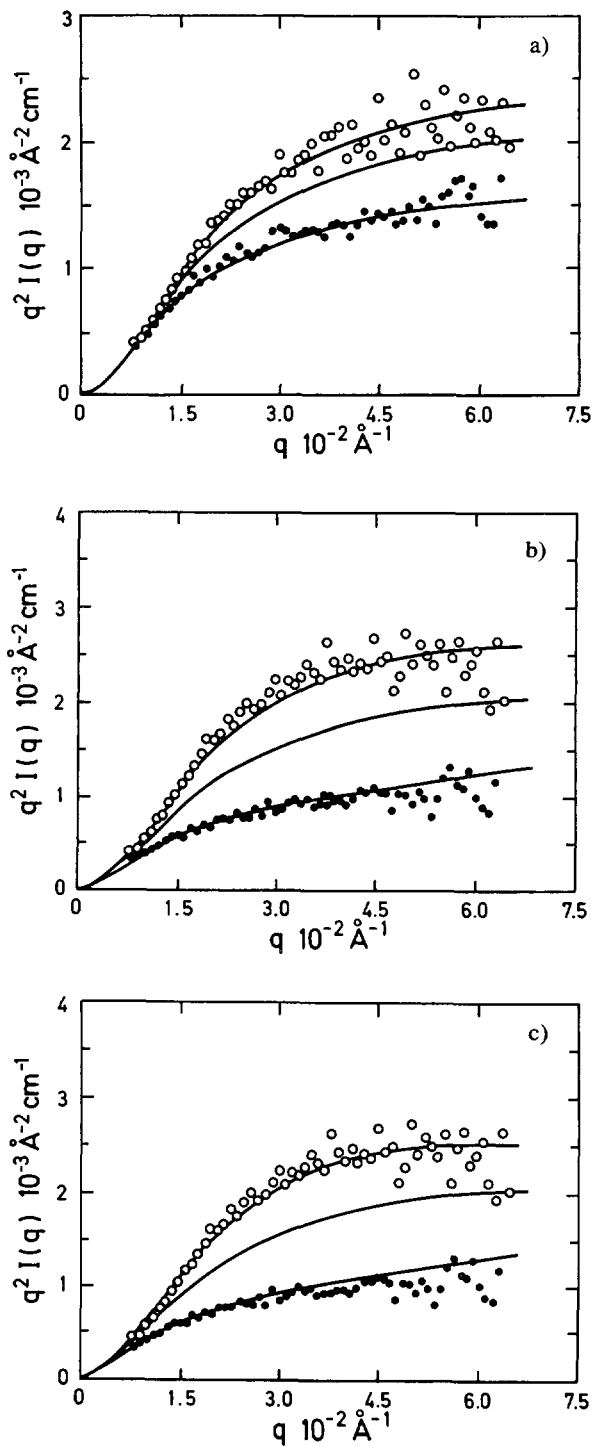
Fig. 5. — Representation $q^2 I(q)$ *versus* q for the scattering of the same mixtures (see caption of Fig. 3) for different elongations λ at the same temperature. The values of the parameters are : a) $\lambda = 1.3$, $T_D = 55\,°C$, $\lambda_p = 1.2$ $p = 5$. b) $\lambda = 1.6$, $T_D = 55\,°C$, $\lambda_p = 1.5$ $p = 10$. c) $\lambda = 2$, $T_D = 55\,°C$, $\lambda_p = 1.6$ $p = 20$.

for the other relaxation times are shown in figure 6a ($t_R = 400$ s) and 6b ($t_R = 1\ 300$ s). In figures 6a and 6b are also shown the best fits to the phantom model ; the corresponding values of λ_p and p are given in table I. Let us notice in figure 6a a strong forward scattering which is not taken into account in the fits because we believe that it is a spurious effect due to the set-up and not to the sample.

For these samples ($t_R = 400$ s and 1 300 s) the effect of the relaxation is clearly seen ; by analogy to amorphous polymers we expect that for longer chains the curves $q^2 I_\perp (q)$ obtained with the same λ and p values would show a maximum. This result, with a shift of the relaxation time scale, is in agreement with the idea of loss of affineness found in the relaxation models of amorphous polymers. A more quantitative comparison requires a more precise determination of the rheological times. We can simply note from the recoverability of the sample that times involved in the deformation are shorter than the terminal time.

Within the accuracy of measurements, the anisotropic X-ray patterns do not change during the relaxation process at this low nematic temperature. Even though the polymer chains are relaxed, the orientation of mesogenic groups remains unchanged : it is normal to the stretching direction with the same half width. *The relaxation of polymer chains does not seem to affect the orientation of mesogens.*

6. Discussion.

We first discuss the relative orientation of the side chain with respect to the stretching axis as observed by X-ray scattering. It is a classical and difficult problem for samples aligned using fiber drawing. It seems that the vast majority of fibers drawn in the SmA phase present side chains perpendicular to the stretch [6, 7]. This observation agrees with the now numerous SANS studies [1c, 23] which show that the side chains are perpendicular to the backbones in the SmA phase, and that the backbones are indeed aligned along the stretching direction. Conversely, fiber samples drawn from the nematic phase lead to both types of orientation according to various factors. For instance, it has been shown in a given series [7] that long spacers induce the perpendicular orientation of the side chains whereas short spacers form the parallel ones. In addition, the parity of the number of methyl groups in the spacer seem to determine the orientation of the side chains in a family of cross linked nematic side chain polymers [3]. It was also shown that the nature (mesogenic or not) of the crosslinks also plays a role in the orientation of mesogenic cores [17]. Our observation of both types of orientation in the nematic phase of a single compound proves that the chemical structure is not the only factor governing the orientation behaviour. For instance, in magnetically oriented samples, the existence of SmA fluctuations in the nematic phase leads to an orientation of the side chains perpendicular to the backbones as demonstrated by SANS [4, 27].

The process of fiber drawing is even more complicated by a possible competition between backbones stretching and nematic flow. The viscoelastic behaviour of the samples is governed not only by the elasticity of the backbone but also by the various viscosities of the nematic phase. A possible interpretation of our results is the following : due to strong SmA fluctuations observed at low temperature (55 °C) the side chains orient perpendicularly to the stretch. Conversely they orient parallel at high temperature because of the nematic natural tendency for this particular spacer and because of a possible nematic flow. Then temperatures around 67 °C represent a cross-over between the two regimes so that no overall orientation is observed.

We now turn to the discussion of the mechanism of stretching of a chain in the nematic phase. This mechanism should explain the pseudo affinity ($\lambda_p < \lambda$) observed for $T = 55$ °C and 67 °C (for $T = 77$ °C, the relaxation is very fast and the results are similar to those of an amorphous polymer in a flow).
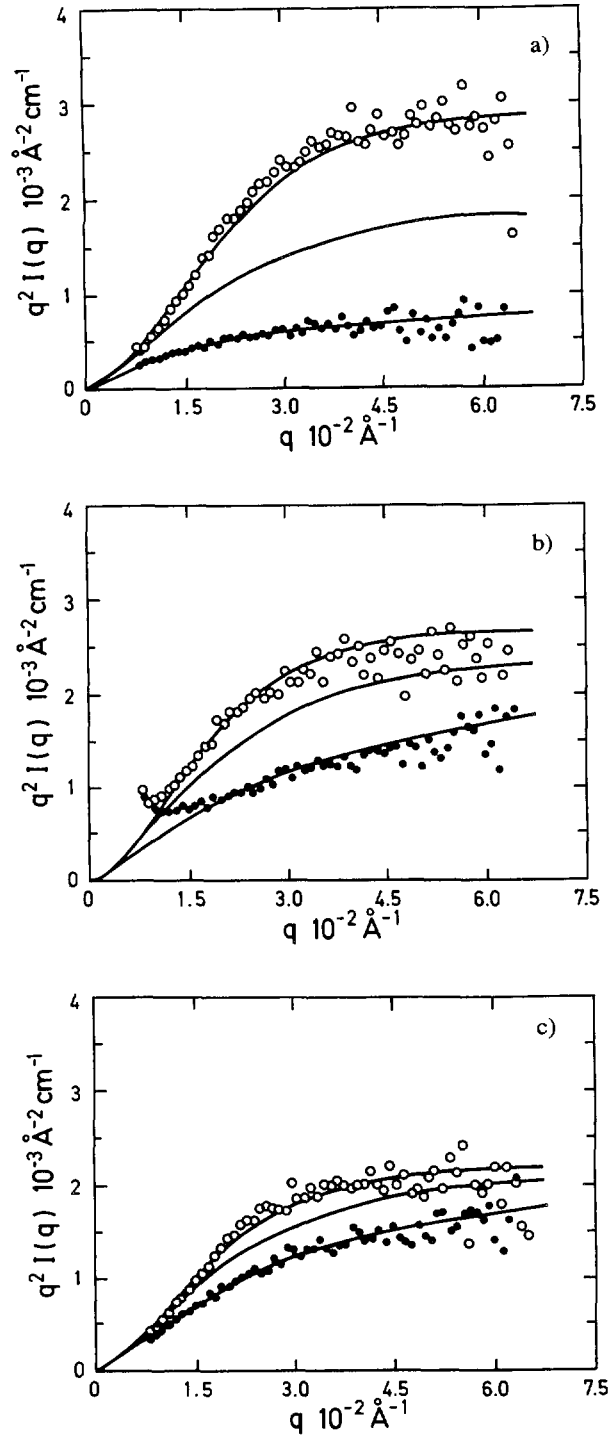
Fig. 6. — Representation $q^2 I(q)$ *versus* q for still the same mixture (see caption of Fig. 3) for the same elongation ratio λ and temperature with different durations of relaxation : a) $\lambda = 3$, $T_D = 55\ °C$, $t_R = 0$, $\lambda_p = 2.05\ p = 10$. b) $\lambda = 3$, $T_D = 55\ °C$, $t_R = 400$ s, $\lambda_p = 1.55\ p = 35$. c) $\lambda = 3$, $T_D = 55\ °C$, $t_R = 1\ 300$ s, $\lambda_p = 1.35\ p = 55$.

A first possibility consists in a decrease of the number of defects (disinclination lines) of the nematic phase just after the beginning of the stretch until formation of a monodomain. After this stage, all the macroscopic stretching would act on the chain. This model is not realistic because, for $\lambda = 1.3$, no noticeable orientation is found by X-ray diffraction while a noticeable orientation of the backbone is observed ($\lambda_p = 1.2$). Moreover $\lambda_p(\lambda)/\lambda$ is a decreasing function of λ.

A second possibility consists in the disappearance of the nematic defects progressively removed by the increasing strain of the chain. This mechanism is consistent with the experimental results. This should explain the weakness of λ_p value with respect to λ, as well as a high anisotropy observed in the largest q range. Such a characteristic behaviour of this polymer for low t_R values ($t_R < 100$ s) is probably due to cooperative effects of the nematic phase. It should also be found with other liquid crystalline polymers.

Let us note that we do not know how to observe the defects by a macroscopic technique well suited to our samples and, besides, due to difficulties in stretching thin samples.

For large t_R the chains seem to relax more similarly to amorphous polymers as large values of p are encountered. The comparison of the variation of λ_p needs a better knowledge of the relaxation time distribution of our polymer.

At this stage the main unresolved question concerns the origin of the effective junctions between the chains. One may think of entanglements between chains as in amorphous polymers, but the chains are short (600 monomers in average). An alternate origin will be specific interactions or entanglements between side chains.

References

[1] a) Keller P., Carvalho B., Cotton J. P., Lambert M., Moussa F., Pépy G., *J. Phys. Lett. France* **46** (1985) 1065 ;
    b) Ohm H. G., Kirste R. G., Oberthür R. C., *Makromol. Chem.* **116** (1988) 1387 ;
    c) Noirez L., Keller P., Cotton J. P., Submitted to *Liq. Cryst.* (1994).

[2] Boué F., *Adv. Polym. Sci.* **82** (1987) 50.

[3] Mitchell G. R., Coulter M., Davis F. J., Guo W., *J. Phys. II France* **2** (1992) 1121.

[4] Davidson P., Noirez L., Cotton J. P., Keller P., *Liq Cryst* **10** (1991) 111.

[5] Boeffel C., Spiess H. W., Side Chain Liquid Crystal Polymers, C. B. M. C. Ardle Ed. (Blachie, Chapman and Hall NY, 1989) p. 224.

[6] Freidzon Y. S., Talroze R. V., Boiko V. I., Kostromin S. G., Shibaev V. P., Plate N. A., *Liq. Cryst.* **3** (1988) 127.

[7] Zentel R., Strobl G. R., *Makromol Chem.* **185** (1984) 2669.

[8] Noël C., in reference [5], p. 159.

[9] Davidson P., Levelut A. M., Keller P., *J Phys France* **46** (1985) 939.

[10] Sutherland H. H., Aliadib Z., Gray G. W., Lacey D., Nestor G., Toyne K. J., *Liq Cryst.* **3** (1988) 1293.

[11] Doi M., Edwards S. F., The Theory of Polymer Dynamics (Clarendon Press, Oxford, 1986).

[12] Cotton J. P., Decker D., Benoit H., Farnoux B., Higgins J., Jannink G., des Cloizeaux J., Ober R., Picot C., *Macromolecules* **7** (1974) 863.

[13] Portugall M., Ringsdorf H., Zentel R., *Makromol. Chem.* **183** (1982) 2311.

[14] Kelker H., Wirzing U., *Mol. Cryst. Liq. Cryst.* **49** (1979) 175.

[15] Boué F., Nierlich M., Jannink G., Ball R. C., *J. Phys. Lett. France* **43** (1982) 589.

[16] Cotton J. P., Neutron X-ray and Light Scattering, P. Lindner and T. Zemb Eds. (Elsevier, 1991) p. 19.

[17] Degert C., Davidson P., Megtert S., Petermann D. and Mauzac M., *Liq. Cryst.* in press.

[18] Lemonnier M., Petermann D. and Megtert S., (1982) CNRS patent 8203344 France.

[19] de Gennes P. G., Scaling concepts in Polymer Physics (Cornell Univ. Press, Ithaca, London, 1979).
[20] Kuhn W., Künzle O., Katchalsky A., *Helv. Chim. Acta XXXI Fasc.* **VI** (1948) 1944.
[21] James H., Guth E., *J. Chem. Phys.* **15** (1947) 669.
[22] Warner M., Edwards S. F., *J. Phys. A* **11** (1978) 1649.
[23] Noirez L., Thesis, Université de Paris-Sud (1989).
[24] Leadbetter A. J., Wrighton P. G., *J. Phys. Colloq. France* **40** (1979) C3-234.
[25] Deutsch M., *Phys. Rev. A* **12** (1991) 264.
[26] Williams M. L., Landel R. F., Ferry J. D., *J. Am. Chem. Soc.* **77** (1955) 3701.
[27] Noirez L., Keller P., Davidson P., Hardouin F., Cotton J. P., *J. Phys France* **49** (1988) 1993.
[28] Davidson P., Levelut A. M., *Liq. Cryst* **11** (1992) 469.